Mechanics of Soft Materials (2024) 6:3
https://doi.org/10.1007/s42558-024-00058-z

ORIGINAL PAPER

An anisotropic hyperelastic strain energy function based on 21 icosahedron fiber distributions

M.B. Rubin[1]

Received: 4 February 2024 / Accepted: 12 April 2024

Abstract
The microscopic Cauchy strain energy for linear elasticity based on the sum of quadratic strain energies due to pair potentials has only 15 material rari-constants. It is shown that the six vectors connecting opposing vertices of a regular icosahedron can be used to develop a strain energy function for general linear elastic anisotropic response with 21 material constants. Specifically, the six strains of material fibers characterized by these vectors are enhanced by 15 fiber distribution strains due to all combinations of distinct pairs of these vectors. These two-vector fiber distributions introduce coupling that is essential to obtaining general anisotropy. The model is generalized for large deformations by replacing the strains with stretches and by using a Fung-type exponential strain energy which couples the responses of the 21 stretches. The resulting nonlinear hyperelastic strain energy function can be used to model the anisotropic hyperelastic response of fibrous tissues.

Keywords Anisotropic · Fiber distributions · Fibrous tissues · Hyperelasticity · Icosahedron · Rari-constants

1 Introduction

The historical introduction in Love [26] describes the microscopic model of elasticity based on pair potentials published in Cauchy's memoir in 1828. The associated strain energy that is a quadratic function of strain based on the sum of energies of pair potentials, each with its own elastic constant, is referred to as the microscopic Cauchy model. It is well known [3, 4, 14, 26, 33, 34] that this microscopic Cauchy model has only 15 independent rari-constants, whereas the general theory of anisotropic elasticity has 21 independent constants. Specifically, the general theory introduces a strain energy Σ per unit mass as a quadratic function of strain

$$\rho_z \Sigma = \frac{1}{2}\mathbf{K} \cdot \boldsymbol{\varepsilon} \otimes \boldsymbol{\varepsilon} = \frac{1}{2} K_{ijk\ell} \varepsilon_{ij} \varepsilon_{k\ell} \,, \tag{1}$$

where ρ_z is the constant zero-stress density. The constant components $K_{ijk\ell}$ of the stiffness tensor $\mathbf{K}$ and the components ε_{ij} of the strain tensor $\boldsymbol{\varepsilon}$, relative to orthonormal base vectors $\mathbf{e}_i$ fixed in the material, are defined so that

$$\mathbf{K} = K_{ijk\ell} \mathbf{e}_i \otimes \mathbf{e}_j \otimes \mathbf{e}_k \otimes \mathbf{e}_\ell \,, \quad \boldsymbol{\varepsilon} = \varepsilon_{ij} \mathbf{e}_i \otimes \mathbf{e}_j \,. \tag{2}$$

✉ M.B. Rubin
mbrubin@tx.technion.ac.il

[1] Faculty of Mechanical Engineering, Technion-Israel Institute of Technology, 32000 Haifa, Israel

Published online: 01 May 2024

Also, the associated symmetric stress tensor $\mathbf{T}$ and its components T_{ij} are given by

$$\mathbf{T} = \rho_z \frac{\partial \Sigma}{\partial \boldsymbol{\varepsilon}} = \mathbf{K} \cdot \boldsymbol{\varepsilon} \,, \quad T_{ij} = K_{ijk\ell} \varepsilon_{k\ell} \,. \tag{3}$$

In addition, throughout this paper, the usual summation convention over repeated lower cased indices ($i = 1, 2, 3$) is implied, $\mathbf{A} \cdot \mathbf{B} = \text{tr}(\mathbf{A}\mathbf{B}^T)$ is the inner product of two second-order tensors ($\mathbf{A}, \mathbf{B}$), and $\mathbf{a} \otimes \mathbf{b}$ is the tensor product of two vectors ($\mathbf{a}, \mathbf{b}$). Details of the inner product of higher-order tensors can be found in Rubin [29]. Moreover, since Σ is a quadratic function of strain and the strain tensor $\boldsymbol{\varepsilon}$ is symmetric, it follows that $K_{ijk\ell}$ satisfies the symmetries

$$K_{jik\ell} = K_{ij\ell k} = K_{k\ell ij} = K_{ijk\ell} \,, \tag{4}$$

which indicates that $K_{ijk\ell}$ has 21 independent constants.

The microscopic Cauchy strain energy is characterized by pair potentials and can be expressed in the form

$$\rho_z \hat{\Sigma} = \frac{1}{2} \sum_{I=1}^{N} \hat{k}_I \hat{\varepsilon}_I^2 = \frac{1}{2} \sum_{I=1}^{N} \hat{k}_I \, (\mathbf{s}_I \otimes \mathbf{s}_I \otimes \mathbf{s}_I \otimes \mathbf{s}_I) \cdot (\boldsymbol{\varepsilon} \otimes \boldsymbol{\varepsilon}) \,, \tag{5}$$

where $\hat{k}_I$ are stiffnesses, the fiber strains $\hat{\varepsilon}_I$ are defined by the unit vectors $\mathbf{s}_I$ characterizing fiber directions, and the associated structural tensors $\mathbf{S}_I$ are defined so that

$$\mathbf{s}_I \cdot \mathbf{s}_I = 1 \,, \quad \mathbf{S}_I = \mathbf{s}_I \otimes \mathbf{s}_I \,, \quad \mathbf{S}_I \cdot \mathbf{I} = 1 \,, \quad \hat{\varepsilon}_I = \mathbf{S}_I \cdot \boldsymbol{\varepsilon} \,. \tag{6}$$

Due to the symmetry of the stiffness tensor in Eq. 5, it is known [3] that the stiffness $K_{ijk\ell}$ of the microscopic Cauchy strain energy function satisfies the additional restrictions

$$K_{ikj\ell} = K_{ijk\ell} \,, \tag{7}$$

which reduces the number of independent constants to 15, called rari-constants. Consequently, the form Eq. 5 cannot describe a general anisotropic response no matter how many pair potentials are considered (large values of N).

The stiffness $K_{ijk\ell}$ can be separated additively into a Cauchy part $K_{i(jk)\ell}$ and its complimentary part $K_{i[jk]\ell}$ defined by Campanella and Tonon [3]

$$\begin{aligned} &K_{ijk\ell} = K_{i(jk)\ell} + K_{i[jk]\ell} \,, \\ &K_{i(jk)\ell} = \frac{1}{2}(K_{ijk\ell} + K_{ikj\ell}) \,, \quad K_{i[jk]\ell} = \frac{1}{2}(K_{ijk\ell} - K_{ikj\ell}) \,. \end{aligned} \tag{8}$$

By definition, this complimentary part $K_{i[jk]\ell}$ is independent of the Cauchy part $K_{i(jk)\ell}$. A number of mathematical aspects of this separation have been discussed by Hehl and Itin [14] and Itin [19–21]. Also, it is known [3] that for linear elasticity, $K_{i[jk]\ell}$ does not contribute to the equations of equilibrium. It was shown by Rubin and Ehret [32] that a general strain energy can be developed by adding to Eq. 5 an additional strain energy that depends on components of $\boldsymbol{\varepsilon}^2$. Moreover, a new spectral representation of the strain energy function was developed by Rubin [31] for general anisotropic response which does not separate the stiffness as in Eq. 8.

One objective of this paper is to develop a new representation of the quadratic strain energy for general anisotropic linear elastic response based on fiber distributions. Instead of focussing on the separation of the stiffness tensor $K_{ijk\ell}$ in Eq. 8, the strain energy function is expressed as the sum of 21 strain energies. In Ciambella and Rubin [6], a fiber distribution Φ_I is defined as a symmetric, positive-definite tensor with unit trace

$$\boldsymbol{\Phi}_I^T = \boldsymbol{\Phi}_I \,, \quad \boldsymbol{\Phi}_I \cdot \mathbf{I} = 1 \,, \quad \boldsymbol{\Phi}_I \cdot \mathbf{s} \otimes \mathbf{s} > 0 \,, \tag{9}$$

where $\mathbf{s}$ is an arbitrary non-zero vector. In this work, the fiber distributions are allowed to be positive semi-definite with

$$\boldsymbol{\Phi}_I \cdot \mathbf{s} \otimes \mathbf{s} \geq 0 \,. \tag{10}$$

Specifically, these fiber distributions are defined by six unit vectors $\mathbf{N}_I$. Six fiber distributions $\mathbf{\Phi}_I \quad (I = 1, 2, \ldots, 6)$ can be considered Dirac distributions each based on a single vector, and the remaining 15 planar-isotropic distributions $\mathbf{\Phi}_I$ $(I = 7, 8, \ldots, 21)$ are defined by all pairs of distinct vectors. Then, the general strain energy function is proposed in the form

$$\rho_z \Sigma = \frac{1}{2} \sum_{I=1}^{21} k_I \varepsilon_I^2 , \quad \varepsilon_I = \mathbf{\Phi}_I \cdot \boldsymbol{\varepsilon} , \tag{11}$$

where k_I are stiffnesses, ε_I are fiber distribution strains, and the associated stress is given by

$$\mathbf{T} = \rho_z \frac{\partial \Sigma}{\partial \boldsymbol{\varepsilon}} = \sum_{I=1}^{21} k_I \varepsilon_I \mathbf{\Phi}_I . \tag{12}$$

The new feature of this representation is the coupling of the strain components ε_{ij} in the fiber distribution strains ε_I $(I = 7, 8, \ldots, 21)$, which is more general than the coupling in the standard fiber strains $\varepsilon_I \quad (I = 1, 2, \ldots, 6)$. This coupling allows the new representation to characterize general anisotropy with 21 independent constants.

Lanir [25] proposed a model for fibrous tissues which is based on stretches of fiber bundles. Anisotropic response can be modeled by introducing non-uniform distributions of the orientation of the fiber bundles; bundle undulation, which causes nonlinear response to fiber stretch; and the stiffness. This model requires integration over all orientations of strains in the direction of a vector defined on the unit sphere. The microplane model for strain-controlled inelastic behavior [2] and the non-affine micro-sphere model of rubber elasticity [27] are examples of other models which require integration of distributions. These structural models attempt to connect the anisotropic response of a material to observable microstructural features. Since there are only five regular polyhedron platonic solids (tetrahedron (4 vertices), octahedron (6 vertices), cube (8 vertices), icosahedron (12 vertices), dodecahedron (20 vertices)), no more than 20 points can be distributed equally spaced on the surface of a sphere. Consequently, numerical integration over the unit sphere can introduce undesired anisotropy and requires a large number of integration points for accuracy [1, 7, 22, 24, 35].

A second objective of this paper is to generalize the model to a nonlinear hyperelastic model for fibrous tissues that is based on 21 affinely deformed fiber distributions. The resulting model is not an approximation of a model based on integration over the surface of a sphere. Instead, it is a phenomenological model for nonlinear anisotropic response based on 21 fiber distribution deformation measures. In this regard, it is mentioned that alternative phenomenological continuum models have been developed using structural tensors to characterize anisotropy [8, 11, 15–18, 23].

An outline of this paper is as follows. Section 2 defines the 21 fiber distributions based on a regular icosahedron. Section 3 and Appendix determine values of the stiffnesses k_I for general anisotropic linear elastic response. Section 4 describes a generalization for nonlinear hyperelastic response with examples that examine undesirable anisotropic response for pure dilatation, isochoric extension, and simple shear. Finally, Section 5 presents a discussion.

2 Fiber distributions based on vertices of a regular icosahedron

The six unit vectors $\mathbf{N}_I$ parallel to opposing vertices of a regular icosahedron (see Fig. 1) were used by Elata and Rubin [9] to study the isotropy of strain energy functions that depend on a finite number of directional strain measures. They were also used by Elata and Rubin [10] to study anisotropy with damage, by Flynn et al. [12] to model the response of fibrous soft tissues, and by Rubin [30] to study anisotropy of a discrete fiber icosahedron model for fibrous tissues. Specifically, $\mathbf{N}_I$ by Rubin [30] are specified by

$$\mathbf{N}_1 = \mathbf{e}_1 , \quad \mathbf{N}_2 = \frac{1}{\sqrt{5}}(\mathbf{e}_1 + 2\mathbf{e}_2) ,$$
$$\mathbf{N}_3 = \frac{1}{\sqrt{5}}\mathbf{e}_1 + \frac{1}{2}\left(1 - \frac{1}{\sqrt{5}}\right)\mathbf{e}_2 + \sqrt{\frac{1}{2}\left(1 + \frac{1}{\sqrt{5}}\right)}\,\mathbf{e}_3 ,$$

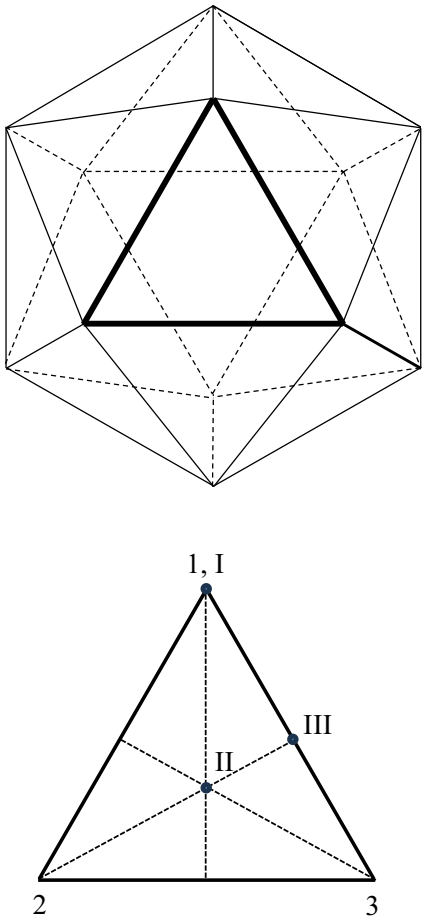

Fig. 1 Sketch of a regular icosahedron and the equilateral triangular defined by $\mathbf{N}_1, \mathbf{N}_2, \mathbf{N}_3$ together with the points I, II, and III defining loading directions

$$\mathbf{N}_4 = \frac{1}{\sqrt{5}}\mathbf{e}_1 - \frac{1}{2}\big(1+\frac{1}{\sqrt{5}}\big)\mathbf{e}_2 + \sqrt{\frac{1}{2}\big(1-\frac{1}{\sqrt{5}}\big)}\,\mathbf{e}_3\,,$$
$$\mathbf{N}_5 = \frac{1}{\sqrt{5}}\mathbf{e}_1 - \frac{1}{2}\big(1+\frac{1}{\sqrt{5}}\big)\mathbf{e}_2 - \sqrt{\frac{1}{2}\big(1-\frac{1}{\sqrt{5}}\big)}\,\mathbf{e}_3\,,$$
$$\mathbf{N}_6 = \frac{1}{\sqrt{5}}\mathbf{e}_1 + \frac{1}{2}\big(1-\frac{1}{\sqrt{5}}\big)\mathbf{e}_2 - \sqrt{\frac{1}{2}\big(1+\frac{1}{\sqrt{5}}\big)}\,\mathbf{e}_3\,. \tag{13}$$

Next, using these vectors, the 21 fiber distributions $\mathbf{\Phi}_I$ are defined by

$$\mathbf{\Phi}_1 = \mathbf{N}_1\otimes\mathbf{N}_1\,,\quad \mathbf{\Phi}_2 = \mathbf{N}_2\otimes\mathbf{N}_2\,,\quad \mathbf{\Phi}_3 = \mathbf{N}_3\otimes\mathbf{N}_3\,,$$
$$\mathbf{\Phi}_4 = \mathbf{N}_4\otimes\mathbf{N}_4\,,\quad \mathbf{\Phi}_5 = \mathbf{N}_5\otimes\mathbf{N}_5\,,\quad \mathbf{\Phi}_6 = \mathbf{N}_6\otimes\mathbf{N}_6\,,$$
$$\mathbf{\Phi}_7 = \tfrac{1}{2}(\mathbf{N}_1\otimes\mathbf{N}_1 + \mathbf{N}_2\otimes\mathbf{N}_2)\,,\quad \mathbf{\Phi}_8 = \tfrac{1}{2}(\mathbf{N}_1\otimes\mathbf{N}_1 + \mathbf{N}_3\otimes\mathbf{N}_3)\,,$$
$$\mathbf{\Phi}_9 = \tfrac{1}{2}(\mathbf{N}_1\otimes\mathbf{N}_1 + \mathbf{N}_4\otimes\mathbf{N}_4)\,,\quad \mathbf{\Phi}_{10} = \tfrac{1}{2}(\mathbf{N}_1\otimes\mathbf{N}_1 + \mathbf{N}_5\otimes\mathbf{N}_5)\,,$$
$$\mathbf{\Phi}_{11} = \tfrac{1}{2}(\mathbf{N}_1\otimes\mathbf{N}_1 + \mathbf{N}_6\otimes\mathbf{N}_6)\,,\quad \mathbf{\Phi}_{12} = \tfrac{1}{2}(\mathbf{N}_2\otimes\mathbf{N}_2 + \mathbf{N}_3\otimes\mathbf{N}_3)\,,$$
$$\mathbf{\Phi}_{13} = \tfrac{1}{2}(\mathbf{N}_2\otimes\mathbf{N}_2 + \mathbf{N}_4\otimes\mathbf{N}_4)\,,\quad \mathbf{\Phi}_{14} = \tfrac{1}{2}(\mathbf{N}_2\otimes\mathbf{N}_2 + \mathbf{N}_5\otimes\mathbf{N}_5)\,,$$
$$\mathbf{\Phi}_{15} = \tfrac{1}{2}(\mathbf{N}_2\otimes\mathbf{N}_2 + \mathbf{N}_6\otimes\mathbf{N}_6)\,,\quad \mathbf{\Phi}_{16} = \tfrac{1}{2}(\mathbf{N}_3\otimes\mathbf{N}_3 + \mathbf{N}_4\otimes\mathbf{N}_4)\,,$$

$$\begin{aligned}
\mathbf{\Phi}_{17} &= \tfrac{1}{2}(\mathbf{N}_3 \otimes \mathbf{N}_3 + \mathbf{N}_5 \otimes \mathbf{N}_5)\,, \quad \mathbf{\Phi}_{18} = \tfrac{1}{2}(\mathbf{N}_3 \otimes \mathbf{N}_3 + \mathbf{N}_6 \otimes \mathbf{N}_6)\,,\\
\mathbf{\Phi}_{19} &= \tfrac{1}{2}(\mathbf{N}_4 \otimes \mathbf{N}_4 + \mathbf{N}_5 \otimes \mathbf{N}_5)\,, \quad \mathbf{\Phi}_{20} = \tfrac{1}{2}(\mathbf{N}_4 \otimes \mathbf{N}_4 + \mathbf{N}_6 \otimes \mathbf{N}_6)\,,\\
\mathbf{\Phi}_{21} &= \tfrac{1}{2}(\mathbf{N}_5 \otimes \mathbf{N}_5 + \mathbf{N}_6 \otimes \mathbf{N}_6)\,.
\end{aligned} \tag{14}$$

From Eqs. 9 and 14, it can be seen that the fiber distribution strains ε_I ($I = 1, 2, \ldots, 6$) are strains of specific material fibers like in Eq. 6, whereas the strains ε_I ($I = 7, 8, \ldots, 21$) are fiber distribution strains based on distributions of all pairs of distinct vectors $\mathbf{N}_I$. Moreover, it is noted that these fiber distributions are different representations of the planar distribution discussed by Holzapfel et al. [16].

3 Determination of the material constants

By equating the strain energy (1) with (11), using the expressions ε_I in Eq. 9 and the fiber distributions $\mathbf{\Phi}_I$ in Eq. 14, the constants k_I can be determined in terms of the stiffnesses $K_{ijk\ell}$ and the results are recorded in Appendix.

3.1 Isotropic response

Using the values of $K_{ijk\ell}$ for isotropic response in Eq. A.1, it can be shown that

$$\begin{aligned}
k_I &= \frac{\mu(7-18\nu)}{2(1-2\nu)} \quad (I = 1, 2, \ldots, 6)\,,\\
k_I &= \frac{\mu(4\nu-1)}{1-2\nu} \quad (I = 7, 8, \ldots, 21)\,,
\end{aligned} \tag{15}$$

where μ is the shear modulus and ν is Poisson's ratio. Notice that for $\nu = 1/4$, this strain energy function reduces to a microscopic Cauchy energy with strains only due to material fibers. The interesting history of Poisson's ratio over two centuries in Greaves [13] discusses this value of ν for the single elastic constant microscopic Cauchy model. Using assumed linear relations between stress and strain components, Cauchy also developed a continuum model for isotropic response with two elastic constants [26]. Furthermore, it can easily be shown that the value $\nu = 1/4$ is consistent with an isotropic linear elastic material with only one independent elastic constant for which Lame's constant $\lambda = \mu$. Moreover, it is noted that k_I are non-negative for $(1/4 \le \nu \le 7/18)$, whereas for other values of ν (i.e. $-1 < \nu < 1/4$ and $7/18 < \nu < 1/2$) in the range $(-1 < \nu < 1/2)$, which ensures that the strain energy function is positive-definite, some of the values of k_I are negative.

3.2 Orthotropic response

Using the values of $K_{ijk\ell}$ for orthotropic response in Eq. A.1, it can be shown that an orthotropic material is characterized by the nine constants

$$\left\{k_1\,, k_2\,, k_3\,, k_4\,, k_7\,, k_8\,, k_{13}\,, k_{16}\,, k_{17}\right\},$$

with the remaining constants given by

$$\begin{aligned}
&k_5 = k_4\,, \quad k_6 = k_3\,, \quad k_{10} = k_9\,, \quad k_{11} = k_8\,, \quad k_{14} = k_{13}\,,\\
&k_{15} = k_{12}\,, \quad k_{20} = k_{17}\,, \quad k_{21} = k_{16}\,,\\
&k_9 = \frac{(\sqrt{5}-1)k_7}{2} + \frac{(3-\sqrt{5})k_8}{2}\,,\\
&k_{12} = -4k_3 + 4k_4 + \frac{(\sqrt{5}-1)k_7}{2} - \frac{(\sqrt{5}-1)k_8}{2} + k_{13} + k_{16} - k_{17}\,,
\end{aligned}$$

$$k_{18} = 2k_2 + (\sqrt{5}-1)k_3 - (\sqrt{5}+1)k_4 - \frac{(\sqrt{5}-1)k_{13}}{2} + \frac{(\sqrt{5}+1)k_{17}}{2}\,,$$
$$k_{19} = 2k_2 - (3+\sqrt{5})k_3 + (\sqrt{5}+1)k_4 + k_7 - k_8 + \frac{(\sqrt{5}+1)k_{13}}{2} + k_{16} - \frac{(\sqrt{5}+1)k_{17}}{2}\,. \tag{16}$$

Notice that if k_I in Eq. 16 are positive, then all k_I will be positive if (k_{12}, k_{18}, k_{19}) are positive. In this regard, (k_2, k_7, k_{16}) can be specified to cause (k_{12}, k_{18}, k_{19}) to be positive. Therefore, a class of orthotropic materials exists for which all k_I are positive.

4 Nonlinear elastic response for fibrous tissues

For the nonlinear theory, the velocity $\mathbf{v}$ of a material point that is located at $\mathbf{x}$ in the current configuration is determined by

$$\mathbf{v} = \dot{\mathbf{x}}\,, \tag{17}$$

where $\dot{(\,)}$ denotes material time differentiation. Also, the total deformation gradient $\mathbf{F}$ from the reference configuration ($\mathbf{F} = \mathbf{I}$) satisfies the evolution equation

$$\dot{\mathbf{F}} = \mathbf{L}\mathbf{F}\,, \tag{18}$$

with the velocity gradient $\mathbf{L}$ and the rate of deformation tensor $\mathbf{D}$ defined by

$$\mathbf{L} = \partial\mathbf{v}/\partial\mathbf{x}\,, \quad \mathbf{D} = \frac{1}{2}(\mathbf{L} + \mathbf{L}^T)\,. \tag{19}$$

Identifying $\mathbf{N}_I$ in Eq. 13 as material fibers, the fiber distribution stretches λ_I and the current affinely deformed fiber distributions $\boldsymbol{\phi}_I$ are defined by

$$\lambda_I = \sqrt{\mathbf{F}\boldsymbol{\Phi}_I\mathbf{F}^T \cdot \mathbf{I}}\,, \quad \boldsymbol{\phi}_I = \frac{\mathbf{F}\boldsymbol{\Phi}_I\mathbf{F}^T}{\lambda_I^2}\,, \tag{20}$$

which satisfy the evolution equations

$$\frac{\dot{\lambda}_I}{\lambda_I} = \boldsymbol{\phi}_I \cdot \mathbf{D}\,, \quad \dot{\boldsymbol{\phi}}_I = \mathbf{L}\boldsymbol{\phi}_I + \boldsymbol{\phi}_I\mathbf{L}^T - 2(\boldsymbol{\phi}_I \cdot \mathbf{D})\boldsymbol{\phi}_I\,. \tag{21}$$

The Fung strain energy by Chuong and Fung [5] is an exponential form of a quadratic strain energy function of the Lagrangian strain. Motivated by this form and modifying the strains, it is possible to propose an exponential Fung-type strain energy for fibrous tissues with 21 fiber distribution stretches in the form

$$\rho_z\Sigma = q\big[\exp\big(\frac{Q}{q}\big) - 1\big]\,, \quad Q = \frac{1}{2}\sum_{I=1}^{21} k_I[\ln(\lambda_I)]^2\,, \tag{22}$$

where the constant $q > 0$ controls nonlinearity and has the dimensions of stress. In this regard, it is noted that for $q \to \infty$, the strain energy reduces to $\rho_z\Sigma = Q$. Moreover, for values of λ_I infinitesimally close to unity, $\rho_z\Sigma$ reduces exactly to the linear elastic form (11). Next, the rate of material dissipation $\mathcal{D}$ for the purely mechanical theory requires

$$\mathcal{D} = \mathbf{T} \cdot \mathbf{D} - \rho\dot{\Sigma} \geq 0\,, \tag{23}$$

where $\mathbf{T}$ is the symmetric Cauchy stress. Also, the current density ρ is related to ρ_z by the conservation of mass equation

$$\rho J = \rho_z\,, \quad J = \det(\mathbf{F}) > 0\,, \tag{24}$$

where J is the total dilatation. Then, using Eqs. 21–23 and the condition that $\mathcal{D}$ vanishes for a hyperelastic material, the Cauchy stress $\mathbf{T}$ and the pressure p are given by

$$\mathbf{T} = J^{-1} \exp\left(\frac{Q}{q}\right) \sum_{I=1}^{21} k_I \ln(\lambda_I) \boldsymbol{\phi}_I \,, \quad p = -\frac{1}{3}(\mathbf{T} \cdot \mathbf{I}) \,. \tag{25}$$

Using the values of k_I in Appendix for the new model based on 21 fiber distribution stretches, it is possible to model general small deformation anisotropy. However, since some of the values of k_I can be negative for general anisotropy, the large deformation response of the model does not necessarily ensure that the strain energy remains non-negative. Moreover, using experimental data to determine values of k_I for large deformation response, it is natural to identify differences in the measured values of k_I from the isotropic values (15) as measures of actual anisotropy. However, it was observed in Rubin [30] that a model based on only $(\boldsymbol{\phi}_I,\ I = 1, 2, \ldots, 6)$ does not predict isotropic response exactly for large deformations. The purpose of this section is to examine the undesirable anisotropy of the new model using the isotropic values (15) by considering examples of pure dilatation, isochoric extension, and simple shear. For all the following examples, k_I are specified by the isotropic values in Eq. 15.

4.1 Pure dilatation

For pure dilatation, the deformation gradient $\mathbf{F}$ is specified by

$$\mathbf{F} = J^{1/3}\mathbf{I} \,, \quad \lambda_I = J^{1/3} \,, \quad \boldsymbol{\phi}_I = \boldsymbol{\Phi}_I \,, \tag{26}$$

and it can be shown using Eqs. 22 and 25 and the results

$$\sum_{I=1}^{6} \boldsymbol{\Phi}_I = 2\mathbf{I} \,, \quad \sum_{I=7}^{21} \boldsymbol{\Phi}_I = 5\mathbf{I} \tag{27}$$

that

$$\begin{aligned} &\mathbf{T} = -p\mathbf{I} \,, \quad p = K \exp\left(\frac{Q}{q}\right) \frac{\ln(J)}{J} \,, \\ &Q = \frac{K}{2}[\ln(J)]^2 \,, \quad K = \frac{2\mu(1+\nu)}{3(1-2\nu)} \,, \end{aligned} \tag{28}$$

where K is the small deformation bulk modulus. As expected the deviatoric stress vanishes and the response is isotropic exactly. Figure 2 shows the influence of q on the dilatational response, with Fig. 2b,c focusing on compression and extension, respectively, to show the different responses more clearly. Moreover, from these figures, it can be seen that the maximum magnitude of the pressure p increases with decreasing values of q and that the response for $q = 100$ [GPa] is very close to that for the limiting value $q = \infty$ [GPa].

4.2 Isochoric extension

For isochoric extension in the unit $\mathbf{p}$ direction, the deformation gradient $\mathbf{F}$ is specified by

$$\mathbf{F} = a\mathbf{p} \otimes \mathbf{p} + \frac{1}{\sqrt{a}}(\mathbf{I} - \mathbf{p} \otimes \mathbf{p}) \,, \quad J = 1 \,, \tag{29}$$

where $a > 0$ is the stretch in the $\mathbf{p}$ direction. Figure 1 shows a sketch of a regular icosahedron and one of its equilateral triangular faces based on vertices defined by $\mathbf{N}_1, \mathbf{N}_2, \mathbf{N}_3$. Due to the symmetry of the icosahedron, the responses for $\mathbf{p} = \mathbf{N}_I$ $(I = 1, 2, \ldots, 6)$ will be identical. Also, the responses for $\mathbf{p}$ piercing identical points in any of the equilateral triangular faces of the icosahedron will be identical. Moreover, due to this symmetry, it is only necessary to consider $\mathbf{p}$ piercing only one of the sub-triangles I-II-2, I-II-3, II-2-3 shown in Fig. 1. Thus, to examine potential anisotropy due to isochoric extension,

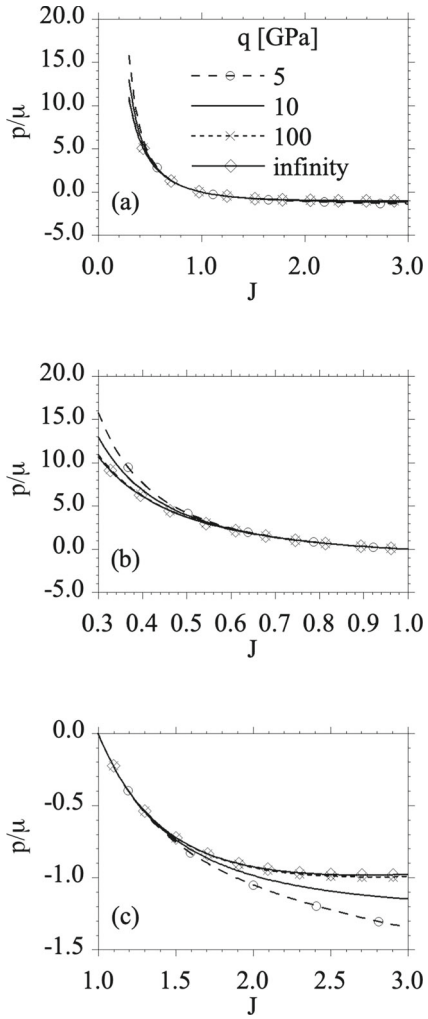

Fig. 2 Pure dilatation: the influence of q on the response

consider unit vectors $\mathbf{p}$ which pierce this triangular face in the triangular region denoted by the points I, II, and III, defined by the unit vectors

$$\begin{aligned} &\text{For E1:} \quad \mathbf{p} = \mathbf{p}_1 = \mathbf{N}_1 \,, \\ &\text{For E2:} \quad \mathbf{p} = \mathbf{p}_2 = \frac{\mathbf{N}_1 + \mathbf{N}_2 + \mathbf{N}_3}{|\mathbf{N}_1 + \mathbf{N}_2 + \mathbf{N}_3|} \,, \\ &\text{For E3:} \quad \mathbf{p} = \mathbf{p}_3 = \frac{\mathbf{N}_1 + \mathbf{N}_3}{|\mathbf{N}_1 + \mathbf{N}_3|} \,. \end{aligned} \tag{30}$$

Also, the axial stress for each loading direction is defined by

$$\sigma = \mathbf{T} \cdot \mathbf{p} \otimes \mathbf{p} \,. \tag{31}$$

For all the following examples, $\nu = 1/3$ and, unless otherwise stated, $q = 10$ (GPa). Figure 3 examines the influence of the constant q on the response for loading in the E1 direction. From this figure, it can be seen that the maximum magnitude of the axial stress σ increases with decreasing values of q and that the response for $q = 100$ [GPa] is very close to that for the limiting value $q = \infty$ [GPa].

The axial stresses σ and the pressures p for isochoric extension in the directions (E1, E2, E3) in Eq. 30, shown in Fig. 4, indicate that the response is not exactly isotropic. Also, it is noted that for extension ($a > 1$), the fiber distributions deform and become more aligned causing increased resistance to extension in the loading direction, whereas for compression ($a < 1$),

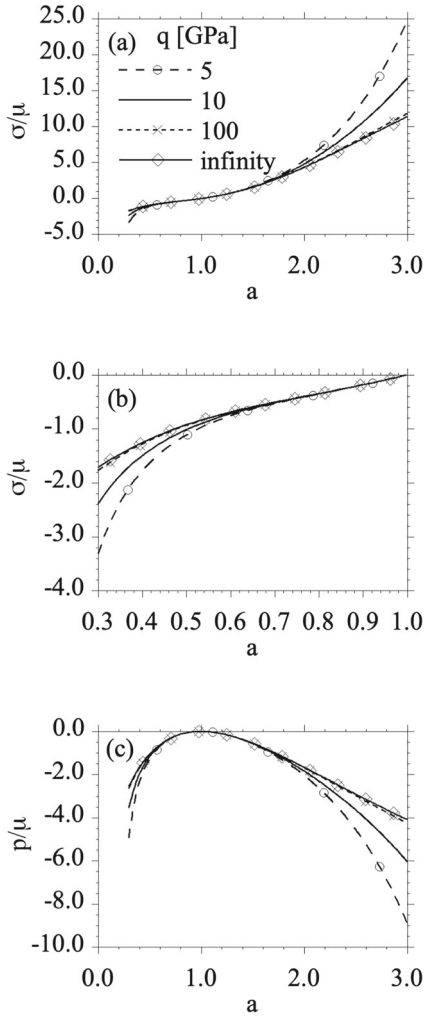

Fig. 3 Isochoric extension: influence of q on the response to loading in the E1 direction

the fiber distributions become flatter and cause increased resistance to expansion normal to the direction of loading, which explains the low values of the axial stress σ for compression.

4.3 Simple shear

For simple shear, the deformation gradient $\mathbf{F}$ is specified by

$$\mathbf{F} = \mathbf{I} + \beta \mathbf{b}_1 \otimes \mathbf{b}_2 \,, \tag{32}$$

where $\mathbf{b}_1$ and $\mathbf{b}_2$ are orthonormal vectors defining the shearing plane with shearing β in the $\mathbf{b}_1$ direction. These vectors are defined for the following two shearing planes:

$$\begin{aligned} \text{For} \quad \text{S1:} \quad & \mathbf{b}_1 = \frac{\mathbf{p}_2 - (\mathbf{p}_2 \cdot \mathbf{b}_2)\mathbf{b}_2}{|\mathbf{p}_2 - (\mathbf{p}_2 \cdot \mathbf{b}_2)\mathbf{b}_2|} \,, \quad \mathbf{b}_2 = \mathbf{N}_1 \,, \\ \text{For} \quad \text{S2:} \quad & \mathbf{b}_1 = \frac{\mathbf{p}_3 - (\mathbf{p}_3 \cdot \mathbf{p}_2)\mathbf{p}_2}{|\mathbf{p}_3 - (\mathbf{p}_3 \cdot \mathbf{b}_2)\mathbf{b}_2|} \,, \quad \mathbf{b}_2 = \mathbf{N}_1 \,. \end{aligned} \tag{33}$$

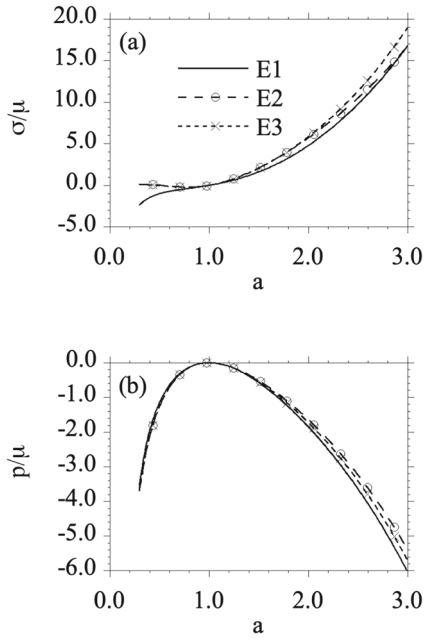

Fig. 4 Isochoric extension: responses to loading in the three directions $E1$, $E2$, and $E3$ in Eq. 30

where $\mathbf{p}_i$ are defined in Eq. 30. Also, $\mathbf{b}_1$ is the unit vector whose projection into the plane of the equilateral triangle in Fig. 1 is directed from the point I to the point II for S1 and directed from the point I to the point III for S2. Figure 5 shows that the response to simple shearing in these two shearing planes is nearly isotropic.

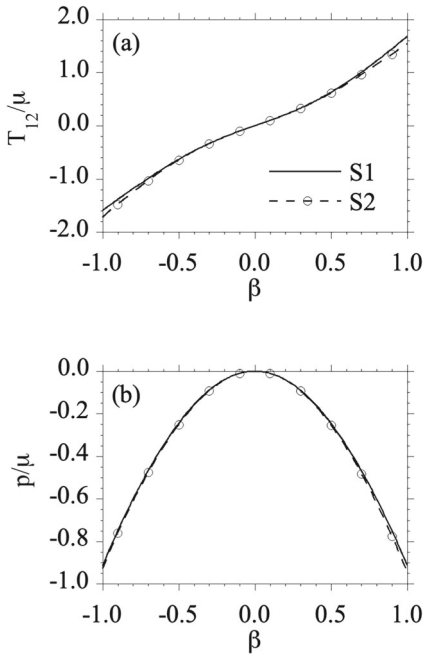

Fig. 5 Simple shear: responses to loading in the two planes S1 and S2 in Eq. 33

5 Discussion

It has been shown that general anisotropic linear elastic response can be characterized by the sum of energies of the 21 strains of fiber distributions of all pairs of the six vectors $\mathbf{N}_I$ in Eq. 13 of a regular icosahedron. To understand the importance of using fiber distribution strains based on two fiber directions to model general anisotropic response, it is recalled from Rubin and Ehret [32] that no matter how many pair potential strains are included in the microscopic Cauchy strain energy (5), there are only 15 independent rari-constants characterizing the strain energy. For example, it was shown by Rubin and Ehret [32] that the dependence of the microscopic Cauchy strain energy on ε_{12}^2 appears only in the combination

$$2\varepsilon_{11}\varepsilon_{22} + \varepsilon_{12}^2 \,. \tag{34}$$

This means that the resistance to ε_{12}^2 cannot be controlled independently. However, the fiber distribution strain ε_7^2 in Eq. 9 for linear elasticity takes the form

$$\varepsilon_7^2 = \frac{25}{4}\left[\varepsilon_{11}^2 + 3\varepsilon_{11}\varepsilon_{12} + 2\varepsilon_{12}\varepsilon_{22} + \varepsilon_{22}^2 + (3\varepsilon_{11}\varepsilon_{22} + \varepsilon_{12}^2)\right], \tag{35}$$

which in combination with the microscopic Cauchy strain energy allows for separate control of the resistances to $\varepsilon_{11}\varepsilon_{22}$ and ε_{12}^2. The extra coupling in the fiber distribution strains ε_I^2 ($I = 7, 8, \ldots, 21$) may be somewhat similar to the extra coupling in a rectangular truss element made of two triangular truss elements that has been stiffened by adding an additional diagonal cross-bar (see Fig. 6).

Replacing the fiber distribution strains ε_I by the logarithm of the fiber distribution stretches λ_I, the strain energy function (11) is generalized for large deformation to take the form Q in Eq. 22. This strain energy function is further generalized by the Fung-type exponential form Σ in Eq. 22.

In microstructural models, like that proposed [25], the distributions of the orientation of the fiber bundles, bundle undulation, and the stiffness are modeled explicitly, with the strain energy proposed as an integral over these distributions. In contrast, the proposed model is phenomenological with the functional forms of the fiber distribution strains in the strain energy function and their associated stiffnesses modeling the combined effects of the distributions in the microstructural models. In both a microstructural model and the fiber distribution model, parameter identification is difficult due to coupled physical effects. However, the proposed model with 21 fiber distributions significantly reduces the computational effort in evaluating the response of the fibrous tissue over that in the microstructural models.

Since the two quantities

$$\sum_{I=1}^{6}[\ln(\lambda_I)]^2 \,, \quad \sum_{I=7}^{21}[\ln(\lambda_I)]^2 \,, \tag{36}$$

cannot be expressed as functions of the invariants of the right Cauchy-Green deformation tensor $\mathbf{C} = \mathbf{F}^T\mathbf{F}$, it follows that the proposed strain energy function cannot characterize nonlinear isotropic elastic response exactly when k_I are specified by the values (15) for isotropic linear elastic response. However, it has been shown that the proposed model, with k_I specified by Eq. 15, is exactly isotropic for small deformations and is nearly isotopic for moderate deformations. The examples indicate that this model based on 21 fiber distribution stretches remains nearly isotropic for a larger range of loading than the model

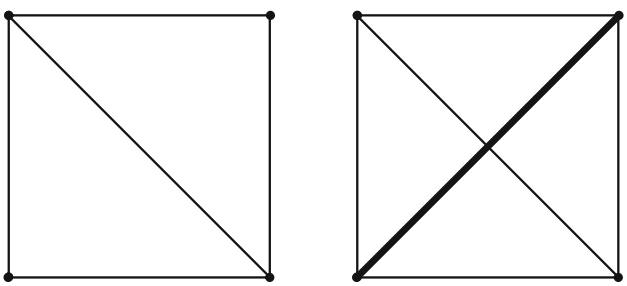

Fig. 6 A truss element stiffened by adding a diagonal cross-bar

in Rubin [30], which used a strain energy function based on the Lagrangian strains of six fiber directions. Furthermore, using (27) and the expression (20) for λ_I, it can be shown that

$$\sum_{I=1}^{6}\lambda_I^2 = 2\mathbf{C}\cdot\mathbf{I}\,,\quad \sum_{I=7}^{21}\lambda_I^2 = 5\mathbf{C}\cdot\mathbf{I}\,. \tag{37}$$

Since $\mathbf{C}\cdot\mathbf{I}$ is the first invariant of $\mathbf{C}$, it follows that exact nonlinear isotropic elastic response can be characterized by a strain energy function that depends on either of these sums.

Modeling the response of fibrous tissues with significant variability requires less accuracy than modeling standard structural materials. For this reason, the undesirable anisotropy exhibited by the proposed model using the isotropic values k_I in Eq. 15 may be insignificant in modeling and understanding the anisotropic response predicted by general values of k_I. In this regard, it may be sufficient to consider anisotropic material response with positive k_I, which ensure that the strain energy function is positive-definite.

Furthermore, it is noted that the logarithmic dependence on the fiber distribution stretches λ_I in Eq. 22 is motivated by the modeling of inelastic response of cardiac muscle [28]. Future work is planned on modeling the anisotropic elastic-inelastic response of fibrous tissues using a generalization of the nonlinear model developed in this paper.

Appendix: Values of the material constants

The material constants k_I can be expressed in terms of the stiffness $K_{ijk\ell}$ by

$$\begin{aligned}
k_1 &= K_{1111} - \frac{7K_{1122}}{4} - \frac{7K_{1133}}{4} + \frac{3K_{2222}}{8} + \frac{3K_{2233}}{4} + \frac{3K_{3333}}{8}\,,\\
k_2 &= -K_{1112} - \frac{3K_{1122}}{4} + \frac{K_{1133}}{4} + 2K_{1212} + 2K_{1222} - 2K_{1233}\\
&\quad + \frac{3K_{2222}}{8} - \frac{5K_{2233}}{4} + \frac{3K_{3333}}{8}\,,\\
k_3 &= \frac{(\sqrt{5}+1)K_{2222}}{16} + \frac{(\sqrt{5}+1)K_{3333}}{16} + \frac{(\sqrt{5}-1)K_{1122}}{8}\\
&\quad - \frac{(3+\sqrt{5})K_{1133}}{8} - \frac{(5+\sqrt{5})K_{2233}}{8} + \frac{(3-\sqrt{5})K_{1212}}{4}\\
&\quad + \frac{(5+\sqrt{5})K_{1313}}{4} + \frac{(5-\sqrt{5})K_{2323}}{4} - \frac{(\sqrt{5}-1)K_{1112}}{4}\\
&\quad - \frac{(\sqrt{5}+1)\sqrt{10-2\sqrt{5}}\,K_{1113}}{8} - \frac{\sqrt{10-2\sqrt{5}}\,K_{1123}}{4} - \frac{K_{1222}}{2}\\
&\quad - \frac{(3+\sqrt{5})\sqrt{10-2\sqrt{5}}\,K_{1322}}{8} - \frac{(\sqrt{5}+1)\sqrt{10-2\sqrt{5}}\,K_{2223}}{8} + \frac{K_{1233}}{2}\\
&\quad + \frac{(3+\sqrt{5})\sqrt{10-2\sqrt{5}}\,K_{1333}}{8} + \frac{(\sqrt{5}+1)\sqrt{10-2\sqrt{5}}\,K_{2333}}{8}\\
&\quad + \frac{\sqrt{10-2\sqrt{5}}\,K_{1213}}{2} + \frac{(\sqrt{5}-1)\sqrt{10-2\sqrt{5}}\,K_{1223}}{4} + \sqrt{5}\,K_{1323}\,,\\
k_4 &= -\frac{(\sqrt{5}-1)K_{2222}}{16} - \frac{(\sqrt{5}-1)K_{3333}}{16} - \frac{(\sqrt{5}+1)K_{1122}}{8}\\
&\quad - \frac{(3-\sqrt{5})K_{1133}}{8} - \frac{(5-\sqrt{5})K_{2233}}{8} + \frac{(3+\sqrt{5})K_{1212}}{4}\\
&\quad + \frac{(5-\sqrt{5})K_{1313}}{4} + \frac{(5+\sqrt{5})K_{2323}}{4} + \frac{(\sqrt{5}+1)K_{1112}}{4}
\end{aligned}$$

$$
\begin{aligned}
&-\frac{\sqrt{10-2\sqrt{5}}\,K_{1113}}{4}+\frac{(\sqrt{5}+1)\sqrt{10-2\sqrt{5}}\,K_{1123}}{8}-\frac{K_{1222}}{2}\\
&+\frac{(\sqrt{5}-1)\sqrt{10-2\sqrt{5}}\,K_{1322}}{8}-\frac{\sqrt{10-2\sqrt{5}}\,K_{2223}}{4}+\frac{K_{1233}}{2}\\
&-\frac{(\sqrt{5}-1)\sqrt{10-2\sqrt{5}}\,K_{1333}}{8}+\frac{\sqrt{10-2\sqrt{5}}\,K_{2333}}{4}\\
&-\frac{(\sqrt{5}+1)\sqrt{10-2\sqrt{5}}\,K_{1213}}{4}+\frac{(3+\sqrt{5})\sqrt{10-2\sqrt{5}}\,K_{1223}}{4}-\sqrt{5}\,K_{1323}\,,\\
k_5 = &-\frac{(\sqrt{5}-1)K_{2222}}{16}-\frac{(\sqrt{5}-1)K_{3333}}{16}-\frac{(\sqrt{5}+1)K_{1122}}{8}\\
&-\frac{(3-\sqrt{5})K_{1133}}{8}-\frac{(5-\sqrt{5})K_{2233}}{8}+\frac{(3+\sqrt{5})K_{1212}}{4}\\
&+\frac{(5-\sqrt{5})K_{1313}}{4}+\frac{(5+\sqrt{5})K_{2323}}{4}+\frac{(\sqrt{5}+1)K_{1112}}{4}\\
&+\frac{\sqrt{10-2\sqrt{5}}\,K_{1113}}{4}-\frac{(\sqrt{5}+1)\sqrt{10-2\sqrt{5}}\,K_{1123}}{8}-\frac{K_{1222}}{2}\\
&-\frac{(\sqrt{5}-1)\sqrt{10-2\sqrt{5}}\,K_{1322}}{8}+\frac{\sqrt{10-2\sqrt{5}}\,K_{2223}}{4}+\frac{K_{1233}}{2}\\
&+\frac{(\sqrt{5}-1)\sqrt{10-2\sqrt{5}}\,K_{1333}}{8}-\frac{\sqrt{10-2\sqrt{5}}\,K_{2333}}{4}\\
&+\frac{(\sqrt{5}+1)\sqrt{10-2\sqrt{5}}\,K_{1213}}{4}-\frac{(3+\sqrt{5})\sqrt{10-2\sqrt{5}}\,K_{1223}}{4}-\sqrt{5}\,K_{1323}\,,\\
k_6 = &\frac{(\sqrt{5}+1)K_{2222}}{16}+\frac{(\sqrt{5}+1)K_{3333}}{16}+\frac{(\sqrt{5}-1)K_{1122}}{8}\\
&-\frac{(3+\sqrt{5})K_{1133}}{8}-\frac{(5+\sqrt{5})K_{2233}}{8}+\frac{(3-\sqrt{5})K_{1212}}{4}\\
&+\frac{(5+\sqrt{5})K_{1313}}{4}+\frac{(5-\sqrt{5})K_{2323}}{4}-\frac{(\sqrt{5}-1)K_{1112}}{4}\\
&+\frac{(\sqrt{5}+1)\sqrt{10-2\sqrt{5}}\,K_{1113}}{8}+\frac{\sqrt{10-2\sqrt{5}}\,K_{1123}}{4}-\frac{K_{1222}}{2}\\
&+\frac{(3+\sqrt{5})\sqrt{10-2\sqrt{5}}\,K_{1322}}{8}+\frac{(\sqrt{5}+1)\sqrt{10-2\sqrt{5}}\,K_{2223}}{8}+\frac{K_{1233}}{2}\\
&-\frac{(3+\sqrt{5})\sqrt{10-2\sqrt{5}}\,K_{1333}}{8}-\frac{(\sqrt{5}+1)\sqrt{10-2\sqrt{5}}\,K_{2333}}{8}\\
&-\frac{\sqrt{10-2\sqrt{5}}\,K_{1213}}{4}-\frac{(\sqrt{5}-1)\sqrt{10-2\sqrt{5}}\,K_{1223}}{4}+\sqrt{5}\,K_{1323}\,,\\
k_7 = &\,4K_{1112}+3K_{1122}-K_{1133}-K_{1222}-K_{1233}-\frac{3K_{2222}}{4}-\frac{K_{2233}}{2}+\frac{K_{3333}}{4}\,,\\
k_8 = &\frac{(\sqrt{5}-1)K_{2222}}{8}-\frac{(3+\sqrt{5})K_{3333}}{8}-\frac{(\sqrt{5}-1)K_{1122}}{2}\\
&+\frac{(3+\sqrt{5})K_{1133}}{2}-\frac{K_{2233}}{2}+(\sqrt{5}-1)K_{1112}\\
&+\frac{(\sqrt{5}+1)\sqrt{10-2\sqrt{5}}\,K_{1113}}{2}+\sqrt{10-2\sqrt{5}}\,K_{1123}-\frac{(\sqrt{5}-1)K_{1222}}{4}
\end{aligned}
$$

$$-\frac{(\sqrt{5}+1)\sqrt{10-2\sqrt{5}}\,K_{1322}}{8}-\frac{\sqrt{10-2\sqrt{5}}\,K_{2223}}{4}-\frac{(\sqrt{5}-1)K_{1233}}{4}$$
$$-\frac{(\sqrt{5}+1)\sqrt{10-2\sqrt{5}}\,K_{1333}}{8}-\frac{\sqrt{10-2\sqrt{5}}\,K_{2333}}{4},$$
$$k_9=-\frac{(\sqrt{5}+1)K_{2222}}{8}-\frac{(3-\sqrt{5})K_{3333}}{8}+\frac{(\sqrt{5}+1)K_{1122}}{2}$$
$$+\frac{(3-\sqrt{5})K_{1133}}{2}-\frac{K_{2233}}{2}-(\sqrt{5}+1)K_{1112}+\sqrt{10-2\sqrt{5}}\,K_{1113}$$
$$-\frac{(\sqrt{5}+1)\sqrt{10-2\sqrt{5}}\,K_{1123}}{2}+\frac{(\sqrt{5}+1)K_{1222}}{4}-\frac{\sqrt{10-2\sqrt{5}}\,K_{1322}}{4}$$
$$+\frac{(\sqrt{5}+1)\sqrt{10-2\sqrt{5}}\,K_{2223}}{8}+\frac{(\sqrt{5}+1)K_{1233}}{4}-\frac{\sqrt{10-2\sqrt{5}}\,K_{1333}}{4}$$
$$+\frac{(\sqrt{5}+1)\sqrt{10-2\sqrt{5}}\,K_{2333}}{8},$$
$$k_{10}=-\frac{(\sqrt{5}+1)K_{2222}}{8}-\frac{(3-\sqrt{5})K_{3333}}{8}+\frac{(\sqrt{5}+1)K_{1122}}{2}$$
$$+\frac{(3-\sqrt{5})K_{1133}}{2}-\frac{K_{2223}}{2}-(\sqrt{5}+1)K_{1112}$$
$$-\frac{(\sqrt{5}-1)\sqrt{10+2\sqrt{5}}\,K_{1113}}{2}+\sqrt{10+2\sqrt{5}}\,K_{1123}+\frac{(\sqrt{5}+1)K_{1222}}{4}$$
$$+\frac{(\sqrt{5}-1)\sqrt{10+2\sqrt{5}}\,K_{1322}}{8}-\frac{\sqrt{10+2\sqrt{5}}\,K_{2223}}{4}+\frac{(\sqrt{5}+1)K_{1233}}{4}$$
$$+\frac{(\sqrt{5}-1)\sqrt{10+2\sqrt{5}}\,K_{1333}}{8}-\frac{\sqrt{10+2\sqrt{5}}\,K_{2333}}{4},$$
$$k_{11}=\frac{(\sqrt{5}-1)K_{2222}}{8}-\frac{(3+\sqrt{5})K_{3333}}{8}-\frac{(\sqrt{5}-1)K_{1122}}{2}$$
$$+\frac{(3+\sqrt{5})K_{1133}}{2}-\frac{K_{2223}}{2}+(\sqrt{5}-1)K_{1112}$$
$$-\frac{(\sqrt{5}+1)\sqrt{10-2\sqrt{5}}\,K_{1113}}{2}-\sqrt{10-2\sqrt{5}}\,K_{1123}-\frac{(\sqrt{5}-1)K_{1222}}{4}$$
$$+\frac{(\sqrt{5}+1)\sqrt{10-2\sqrt{5}}\,K_{1322}}{8}+\frac{\sqrt{10-2\sqrt{5}}\,K_{2223}}{4}-\frac{(\sqrt{5}-1)K_{1233}}{4}$$
$$+\frac{(\sqrt{5}+1)\sqrt{10-2\sqrt{5}}\,K_{1333}}{8}+\frac{\sqrt{10-2\sqrt{5}}\,K_{2333}}{4},$$
$$k_{12}=-\frac{3(\sqrt{5}-1)K_{2222}}{8}-\frac{(3+\sqrt{5})K_{3333}}{8}+\frac{(2+\sqrt{5})K_{2233}}{2}$$
$$+(\sqrt{5}-1)K_{1212}+\frac{(\sqrt{5}-1)K_{1222}}{4}+\frac{3(\sqrt{5}+1)\sqrt{10-2\sqrt{5}}\,K_{1322}}{8}$$
$$+\frac{3\sqrt{10-2\sqrt{5}}\,K_{2223}}{4}+\frac{(7+\sqrt{5})\,K_{1233}}{4}-\frac{(\sqrt{5}+1)\sqrt{10-2\sqrt{5}}\,K_{1333}}{8}$$
$$-\frac{\sqrt{10-2\sqrt{5}}\,K_{2333}}{4}+\frac{(\sqrt{5}+1)\sqrt{10-2\sqrt{5}}\,K_{1213}}{2}+\sqrt{10-2\sqrt{5}}\,K_{1223},$$
$$k_{13}=\frac{3(\sqrt{5}+1)K_{2222}}{8}-\frac{(3-\sqrt{5})K_{3333}}{8}-\frac{(\sqrt{5}-2)K_{2233}}{2}$$

$$
\begin{aligned}
&-(\sqrt{5}+1)K_{1212}-\frac{(\sqrt{5}+1)K_{1222}}{4}+\frac{3\sqrt{10-2\sqrt{5}}\,K_{1322}}{4}\\
&\quad-\frac{3(\sqrt{5}+1)\sqrt{10-2\sqrt{5}}\,K_{2223}}{8}+\frac{(7-\sqrt{5})K_{1233}}{4}-\frac{\sqrt{10-2\sqrt{5}}\,K_{1333}}{4}\\
&\quad+\frac{(\sqrt{5}+1)\sqrt{10-2\sqrt{5}}\,K_{2333}}{8}+\sqrt{10-2\sqrt{5}}\,K_{1213}-\frac{(\sqrt{5}+1)\sqrt{10-2\sqrt{5}}\,K_{1223}}{2},\\
k_{14}=&\frac{3(\sqrt{5}+1)K_{2222}}{8}-\frac{(3-\sqrt{5})K_{3333}}{8}-\frac{(\sqrt{5}-2)K_{2233}}{2}\\
&-(\sqrt{5}+1)K_{1212}-\frac{(\sqrt{5}+1)K_{1222}}{4}-\frac{3\sqrt{10-2\sqrt{5}}\,K_{1322}}{4}\\
&\quad+\frac{3(\sqrt{5}+1)\sqrt{10-2\sqrt{5}}\,K_{2223}}{8}+\frac{(7-\sqrt{5})K_{1233}}{4}+\frac{\sqrt{10-2\sqrt{5}}\,K_{1333}}{4}\\
&\quad-\frac{(\sqrt{5}+1)\sqrt{10-2\sqrt{5}}\,K_{2333}}{8}-\sqrt{10-2\sqrt{5}}\,K_{1213}+\frac{(\sqrt{5}+1)\sqrt{10-2\sqrt{5}}\,K_{1223}}{2},\\
k_{15}=&-\frac{3(\sqrt{5}-1)K_{2222}}{8}-\frac{(3+\sqrt{5})K_{3333}}{8}+\frac{(\sqrt{5}+2)K_{2233}}{2}\\
&+(\sqrt{5}-1)K_{1212}+\frac{(\sqrt{5}-1)K_{1222}}{4}-\frac{3(\sqrt{5}+1)\sqrt{10-2\sqrt{5}}\,K_{1322}}{8}\\
&\quad-\frac{3\sqrt{10-2\sqrt{5}}\,K_{2223}}{4}+\frac{(7+\sqrt{5})K_{1233}}{4}+\frac{(\sqrt{5}+1)\sqrt{10-2\sqrt{5}}\,K_{1333}}{8}\\
&\quad+\frac{\sqrt{10-2\sqrt{5}}\,K_{2333}}{4}-\frac{(\sqrt{5}+1)\sqrt{10-2\sqrt{5}}\,K_{1213}}{2}-\sqrt{10-2\sqrt{5}}\,K_{1223},\\
k_{16}=&-\frac{K_{2222}}{4}+\frac{K_{3333}}{4}+K_{2233}-K_{1212}+\sqrt{5}\,K_{1313}-\sqrt{5}\,K_{2323}+K_{1222}\\
&+\frac{\sqrt{10-2\sqrt{5}}\,K_{1322}}{2}+\frac{(3+\sqrt{5})\sqrt{10-2\sqrt{5}}\,K_{2223}}{8}-2K_{1233}\\
&+\frac{(\sqrt{5}+1)\sqrt{10-2\sqrt{5}}\,K_{1333}}{4}-\frac{(1+3\sqrt{5})\sqrt{10-2\sqrt{5}}\,K_{2333}}{8}\\
&\quad-\sqrt{10-2\sqrt{5}}\,K_{1213}-\frac{(3+\sqrt{5})\sqrt{10-2\sqrt{5}}\,K_{1223}}{4}-\sqrt{5}\,K_{1323},\\
k_{17}=&-\frac{K_{2222}}{4}+\frac{K_{3333}}{4}+K_{2233}-K_{1212}-\sqrt{5}\,K_{1313}+\sqrt{5}\,K_{2323}+K_{1222}\\
&+\frac{(\sqrt{5}+1)\sqrt{10-2\sqrt{5}}\,K_{1322}}{4}+\frac{(\sqrt{5}-1)\sqrt{10-2\sqrt{5}}\,K_{2223}}{8}-2K_{1233}\\
&-\frac{\sqrt{10-2\sqrt{5}}\,K_{1333}}{2}+\frac{(7+\sqrt{5})\sqrt{10-2\sqrt{5}}\,K_{2333}}{8}\\
&\quad-\frac{(\sqrt{5}+1)\sqrt{10-2\sqrt{5}}\,K_{1213}}{2}-\frac{(\sqrt{5}-1)\sqrt{10-2\sqrt{5}}\,K_{1223}}{4}+\sqrt{5}\,K_{1323},\\
k_{18}=&\frac{(3-\sqrt{5})K_{2222}}{8}+\frac{(7+3\sqrt{5})K_{3333}}{8}-\frac{(\sqrt{5}+1)K_{2233}}{4}\\
&\quad+\frac{(3-\sqrt{5})K_{1212}}{2}-\frac{(5+\sqrt{5})K_{1313}}{2}-\frac{(5-\sqrt{5})K_{2323}}{2}\\
&\quad-\frac{(3-\sqrt{5})K_{1222}}{2}+\frac{(\sqrt{5}+1)K_{1233}}{2}-2\sqrt{5}\,K_{1323},
\end{aligned}
$$

$$
\begin{aligned}
k_{19} &= \frac{(3+\sqrt{5})K_{2222}}{8} - \frac{(3\sqrt{5}-7)K_{3333}}{8} + \frac{(\sqrt{5}-1)K_{2233}}{4} \\
&+ \frac{(3+\sqrt{5})K_{1212}}{2} - \frac{(5-\sqrt{5})K_{1313}}{2} - \frac{(5+\sqrt{5})K_{2323}}{2} \\
&- \frac{(3+\sqrt{5})K_{1222}}{2} - \frac{(\sqrt{5}-1)K_{1233}}{2} + 2\sqrt{5}\,K_{1323}\,, \\
k_{20} &= -\frac{K_{2222}}{4} + \frac{K_{3333}}{4} + K_{2233} - K_{1212} - \sqrt{5}\,K_{1313} + \sqrt{5}\,K_{2323} + K_{1222} \\
&- \frac{(\sqrt{5}+1)\sqrt{10-2\sqrt{5}}\,K_{1322}}{4} - \frac{(\sqrt{5}-1)\sqrt{10-2\sqrt{5}}\,K_{2223}}{8} - 2K_{1233} \\
&+ \frac{\sqrt{10-2\sqrt{5}}\,K_{1333}}{2} - \frac{(7+\sqrt{5})\sqrt{10-2\sqrt{5}}\,K_{2333}}{8} \\
&+ \frac{(\sqrt{5}+1)\sqrt{10-2\sqrt{5}}\,K_{1213}}{2} + \frac{(\sqrt{5}-1)\sqrt{10-2\sqrt{5}}\,K_{1223}}{4} + \sqrt{5}\,K_{1323}\,, \\
k_{21} &= -\frac{K_{2222}}{4} + \frac{K_{3333}}{4} + K_{2233} - K_{1212} + \sqrt{5}\,K_{1313} - \sqrt{5}\,K_{2323} + K_{1222} \\
&- \frac{\sqrt{10-2\sqrt{5}}\,K_{1322}}{2} - \frac{(3+\sqrt{5})\sqrt{10-2\sqrt{5}}\,K_{2223}}{8} - 2K_{1233} \\
&- \frac{(\sqrt{5}+1)\sqrt{10-2\sqrt{5}}\,K_{1333}}{4} + \frac{(1+3\sqrt{5})\sqrt{10-2\sqrt{5}}\,K_{2333}}{8} \\
&+ \sqrt{10-2\sqrt{5}}\,K_{1213} + \frac{(3+\sqrt{5})\sqrt{10-2\sqrt{5}}\,K_{1223}}{4} - \sqrt{5}\,K_{1323}\,.
\end{aligned}
\tag{A.1}
$$

Funding Open access funding provided by Technion - Israel Institute of Technology.

Data Availability Data sharing is not applicable to this article as no datasets were generated or analyzed during the current study.

Declarations

Conflict of interest The author declares no competing interests.

References

1. Bažant, P., Oh, B.H.: Efficient numerical integration on the surface of a sphere. ZAMM-J. Appl. Math. Mech./Zeitschrift Angewandte Math. Mech. **66**(1), 37–49 (1986)
2. Bažant, Z.: Microplane model for strain controlled inelastic behaviour. In: Desai, C., Gallagher, R.G. (eds.) Mechanics of Engineering Materials, Ch. 3, pp. 45–59. Wiley (1984)
3. Campanella, A., Tonon, M.L.: A note on the Cauchy relations. Meccanica **29**, 105–108 (1994)
4. Capecchi, D., Ruta, G.: The theory of elasticity in the 19th century. In: Strength of materials and theory of elasticity in 19th century italy. Advanced Structured Materials, vol. 52, pp. 105–108 (2015)
5. Chuong, C.J., Fung, Y.C.: Three-dimensional stress distribution in arteries. ASME J. Biomech. Eng. **105**, 268–274 (1983)
6. Ciambella, J., Rubin, M.B.: An elastic-viscoplastic model with non-affine deformation and rotation of a distribution of embedded fibres. Eur. J. Mech. A/Solids **100**, 104985 (2023)
7. Ehret, A.E., Itskov, M., Schmid, H.: Numerical integration on the sphere and its effect on the material symmetry of constitutive equations–a comparative study. Int. J. Numer. Methods Eng. **81**(2), 189–206 (2010)

8. Ehret, A.E., Itskov, M., Weinhold, G.W.: A micromechanically motivated model for the viscoelastic behaviour of soft biological tissues at large strains. Il Nuovo Cimento C-Geophys. Space Phys. **32**(1), 73–80 (2009)
9. Elata, D., Rubin, M.B.: Isotropy of strain energy functions which depend only on a finite number of directional strain measures. ASME J. Appl. Mech. **61**, 284–289 (1994)
10. Elata, D., Rubin, M.B.: A new representation for the strain energy of anisotropic elastic materials with application to damage evolution in brittle materials. Mech. Mater. **19**, 171–192 (1995)
11. Flynn, C., Rubin, M.B.: An anisotropic discrete fibre model based on a generalised strain invariant with application to soft biological tissues. Int. J. Eng. Sci. **60**, 66–76 (2012)
12. Flynn, C., Rubin, M.B., Nielsen, P.: A model for the anisotropic response of fibrous soft tissues using six discrete fibre bundles. Int. J. Numer. Method. Biomed. Eng. **27**(11), 1793–1811 (2011)
13. Greaves, G.N.: Poisson's ratio over two centuries: challenging hypotheses. Notes Rec. R. Soc. **67**(1), 37–58 (2013)
14. Hehl, F.W., Itin, Y.: The Cauchy relations in linear elasticity theory. J. Elast. **66**, 185–192 (2002)
15. Holzapfel, G.A., Gasser, T.C., Ogden, R.W.: A new constitutive framework for arterial wall mechanics and a comparative study of material models. J. Elast. Phys. Sci. Solids **61**(1), 1–48 (2000)
16. Holzapfel, G.A., Niestrawska, J.A., Ogden, R.W., Reinisch, A.J., Schriefl, A.J.: Modelling non-symmetric collagen fibre dispersion in arterial walls. J. R. Soc. Interface **12**(106), 20150188 (2015)
17. Holzapfel, G.A., Ogden, R.W.: Constitutive modelling of arteries. Proc. R. Soc. A: Math. Phys. Eng. Sci. **466**(2118), 1551–1597 (2010)
18. Holzapfel, G.A., Ogden, R.W., Sherifova, S.: On fibre dispersion modelling of soft biological tissues: a review. Proc. R. Soc. A **475**(2224), 20180736 (2019)
19. Itin, Y.: Quadratic invariants of the elasticity tensor. J. Elast. **125**, 39–62 (2016)
20. Itin, Y.: Irreducible matrix resolution for symmetry classes of elasticity tensors. Math. Mech. Solids **25**(10), 1873–1895 (2020)
21. Itin, Y.: Cauchy relations in linear elasticity: algebraic and physics aspects. arXiv:2304.09579 (2023)
22. Itskov, M.: On the accuracy of numerical integration over the unit sphere applied to full network models. Comput. Mech. **57**(5), 859–865 (2016)
23. Itskov, M., Ehret, A.E.: A universal model for the elastic, inelastic and active behaviour of soft biological tissues. GAMM-Mitteilungen **32**(2), 221–236 (2009)
24. Itskov, M., Ehret, A.E., Dargazany, R.: A full-network rubber elasticity model based on analytical integration. Math. Mech. Solids **15**(6), 655–671 (2010)
25. Lanir, Y.: Constitutive equations for fibrous connective tissues. J. Biomech. **16**(1), 1–12 (1983)
26. Love, A.E.: Mathematical theory of elasticity. Dover (1960)
27. Miehe, C., Göktepe, S., Lulei, F.: A micro-macro approach to rubber-like materials-part I: the non-affine micro-sphere model of rubber elasticity. J. Mech. Phys. Solids **52**(11), 2617–2660 (2004)
28. Rubin, M.B.: A viscoplastic model for the active component in cardiac muscle. Biomech. Model. Mechanobiol. **15**(4), 965–982 (2016)
29. Rubin, M.B.: Continuum mechanics with Eulerian formulations of constitutive equations. Springer Nature (2021)
30. Rubin, M.B.: Anisotropy of a discrete fiber icosahedron model for fibrous tissues exhibited for large deformations. Mech. Soft Mater. **4**, 2 (2022)
31. Rubin, M.B.: A new spectral representation of the strain energy function for linear anisotropic elasticity with a generalization for damage. Int. J. Eng. Sci. **193**, 103916 (2023)
32. Rubin, M.B., Ehret, A.E.: Invariants for rari-and multi-constant theories with generalization to anisotropy in biological tissues. J. Elast. **133**(1), 119–127 (2018)
33. Todhunter, I., Pearson, K.: A history of the theory of elasticity and of the strength of materials, from Galileo to Lord Kelvin, vol. I. Dover, Galilei to Saint-Venant (1960)
34. Vannucci, P.: Anisotropic elasticity. In: Wriggers, P., P Eberhard, E. (eds.) Lecture notes in applied and computational mechanics, vol. 85. Springer (2017)
35. Verron, E.: Questioning numerical integration methods for microsphere (and microplane) constitutive equations. Mech. Mater. **89**, 216–228 (2015)